Ceramide kinase promotes Ca^{2+} signaling near IgG-opsonized targets and enhances phagolysosomal fusion in COS-1 cells[S]

Vania Hinkovska-Galcheva,[1,*,†] Andrea Clark,[§] Susan VanWay,[†] Ji-Biao Huang,[§] Miki Hiraoka,[**] Akira Abe,[**] Michael Borofsky,[*] Robin G. Kunkel,[††] Thomas Shanley,[†] James A. Shayman,[**] Frederick Lanni,[§§] Howard R. Petty,[§,***] and Laurence A. Boxer[*]

Department of Pediatrics, Division of Hematology/Oncology,* Department of Pediatrics, Division of Critical Care Medicine,† Department of Ophthalmology and Visual Science,§ Department of Internal Medicine, Division of Nephrology,** Department of Pathology,†† and Department of Microbiology and Immunology,*** University of Michigan Medical School, Ann Arbor, MI 48109; and Department of Biological Sciences,§§ Carnegie-Mellon University, Pittsburgh, PA 15213

Abstract Ceramide-1-phosphate (C1P) is a novel bioactive sphingolipid formed by the phosphorylation of ceramide catalyzed by ceramide kinase (CERK). In this study, we evaluated the mechanism by which increased C1P during phagocytosis enhances phagocytosis and phagolysosome formation in COS-1 cells expressing hCERK. Stable transfectants of COS-1 cells expressing FcγRIIA or both FcγRIIA/hCERK expression vectors were created. Cell fractionation studies demonstrated that hCERK and the transient receptor potential channel (TRPC-1) were enriched in caveolae fractions. Our data establish that both CERK and TRPC-1 localize to the caveolar microdomains during phagocytosis and that CERK also colocalizes with EIgG in FcγRIIA/hCERK-bearing COS-1 cells. Using high-speed fluorescence microscopy, FcγRIIA/hCERK transfected cells displayed Ca^{2+} sparks around the phagosome. In contrast, cells expressing FcγRIIA under identical conditions displayed little periphagosomal Ca^{2+} signaling. The enhanced Ca^{2+} signals were accompanied by enhanced phagolysosome formation. However, the addition of pharmacological reagents that inhibit store-operated channels (SOCs) reduced the phagocytic index and phagolysosomal fusion in hCERK transfected cells.[JLR] The higher Ca^{2+} signal observed in hCERK transfected cells as well as the fact that CERK colocalized with EIgG during phagocytosis support our hypothesis that Ca^{2+} signaling is an important factor for increasing phagocytosis and is regulated by CERK in a manner that involves SOCs/TRPCs.—Hinkovska-Galcheva, V., A. Clark, S. VanWay, J-B. Huang, M. Hiraoka, A. Abe, M. Borofsky, R. G. Kunkel, T. Shanley, J. A. Shayman, F. Lanni, H. R. Petty, and L. A. Boxer. Ceramide kinase promotes Ca^{2+} signaling near IgG-opsonized targets and enhances phagolysosomal fusion in COS-1 cells. *J. Lipid Res.* 2008. **49:** 531–542.

Supplementary key words immunoglobulin G • ceramide-1-phosphate • store operated channels • transient potential channel • phagocytosis

Phagocytosis plays an essential role in host-defense mechanisms (1). Phagocytosis is often triggered by the interaction of target-bound opsonins with specific receptors on the surface of phagocytes. These receptors include the Fc receptors, which bind to the Fc portion of immunoglobulins (2), and the complement receptors (3), which bind to complement deposited on targets. Activation of these receptors leads to a reorganization of the plasma membrane that profoundly affects the function of phagocytes. The plasma membrane forms pseudopods that extend around an extracellular particle followed by their fusion to form a membrane-bound intracellular vesicle, the phagosome. As the process of phagocytosis proceeds, cytoplasmic granules fuse with the phagosome membrane to deliver hydrolytic and antibacterial enzymes to the phagosome (4). Phagolysosome formation is dependent upon intracellular Ca^{2+} and requires the activity of a complex containing docking and fusion proteins (5, 6).

Ca^{2+} is a ubiquitous intracellular messenger controlling a diverse range of cellular processes, such as gene transcription, muscle contraction, cell proliferation, and apoptosis (7). Cytosolic Ca^{2+} signaling occurs through both Ca^{2+} release from intracellular stores and Ca^{2+} entry from the extracellular environment. Membrane Ca^{2+} channels can be *1*) voltage operated channels (VOCs), *2*) non-voltage-gated Ca^{2+}-permeable channels (NVGCs), *3*) receptor-operated Ca^{2+} channels (ROCs), *4*) store-operated channels (SOCs), and *5*) small molecule-operated channels (SMOCs). VOCs are used largely by excitable cell types such as muscle and neuronal cells, in which they are activated by plasma membrane depolariza-

tion. The NVGCs include ion channels activated by the binding of extracellular and intracellular messengers, mechanical stress, or the depletion of intracellular calcium stores. ROCs are structurally and functionally diverse channels found on secretory cells and nerve terminals. SMOCs are activated by a number of small messenger molecules. There is evidence that Ca^{2+} channels can be activated by intracellular lipid messengers, such as diacylglycerol (8) and arachidonic acid (9). SOCs are opened after the depletion of internal Ca^{2+} stores. As many cell types have been shown to have enhanced Ca^{2+} entry after Ca^{2+} pool depletion, SOCs are one of the most frequently encountered plasma membrane Ca^{2+} channels. At present, the best candidates for the molecular identity of SOCs are homologs of the transient receptor potential channel (TRPC) that functions in *Drosophila* photoreception (10). The mechanisms by which SOCs operate are largely unknown. Recent studies have indicated that members of the TRP family of ion channels can function as Ca^{2+} influx channels in excitable and nonexcitable tissues (10).

Sphingolipids, including sphingosine, sphingosine-1-phosphate, and sphingosylphosphorylcholine, have diverse effects on the regulation of intracellular free calcium concentration in nonexcitable and excitable cells (11, 12). Many of these effects are mediated by G-protein-coupled plasma membrane receptors for sphingolipids (12, 13). Ceramide-1-phosphate (C1P) has also emerged as a putative modulator of cellular functions (14). According to some reports, C1P itself does not modulate intracellular free calcium concentration (15, 16). Others have shown that C1P enhances store-operated Ca^{2+} entry into thyroid cells (17). C1P does not affect Ca^{2+} mobilization in mouse fibroblasts (18, 19), neutrophils (20), or A549 cells (15). A truncated C1P with a C_2 ceramide induces Ca^{2+} mobilization in calf pulmonary artery endothelial cells (21). Therefore, the effect of C1P in Ca^{2+} regulation remains controversial.

Most studies to date have examined the mechanism of action of C1P by exogenous addition to cells. The cloning of ceramide kinase (CERK) provides a new tool to study the role of C1P in cell signaling. We have found that transfection of COS-1 cells with human ceramide kinase (hCERK) affected Ca^{2+} signaling events. In this study, we identified calcium signals in the vicinity of phagosomes during phagocytosis by introducing the hCERK gene into COS-1 cells. To ascertain whether C1P was also formed during phagocytosis, hCERK transfected COS-1 cells were labeled with the ceramide precursor [^{3}H]D-*erythro*-sphingosine. The amount of radioactive C1P increased by 3-fold in the hCERK transfected cells compared with the vector control cells and nontransfected FcγRIIA cells. These transfections did not have any significant effect on cell viability and growth and, as stated above, led to an increase in CERK activity and C1P levels during stimulation with EIgG (22). Our studies suggest a novel role for C1P in Ca^{2+} signaling and contribute to our understanding of the role of increased Ca^{2+} signals in promoting phagocytosis and phagolysosomal fusion.

METHODS

Materials

The proteinase inhibitors pepstatin and leupeptin, mibefradil, $CdCl_2$, and rabbit anti-goat antibody were obtained from Sigma. LysoTracker Red DND-99 Indo-1-AM was obtained from Molecular Probes, Inc. (Eugene, OR). Carboxyamido-triazole (CAI) was the generous gift of Dr. R. Schultz (Drug Synthesis and Chemistry Branch, Developmental Therapeutics Program, Division of Cancer Treatment and Diagnosis, National Cancer Institute, Bethesda, MD). The SOC antagonist 1-(β-[3-(4-methoxyphenyl)propoxy]4-methoxyphenethyl)-1H-imidazole (SKF96365) was purchased from Biomol (Plymouth Meeting, PA). Western blotting detection reagents and horseradish peroxidase-conjugated sheep anti-mouse antibody were acquired from Amersham Biosciences (Piscataway, NJ). Goat anti-rabbit IgG horseradish peroxidase and FITC-conjugated caveolin-1 were purchased from Santa Cruz Biotechnology (Santa Cruz, CA). Polyclonal antibody against caveolin-1 and rabbit anti-TRPC-1 antibody were purchased from Chemicon International (Temecula, CA). Purified rabbit CERK polyclonal antibody was purchased from Abgent (San Diego, CA). Dulbecco's modified Eagle's medium, opti-MEM medium, trypsin EDTA, L-glutamine, penicillin/streptomycin, and geneticin (G-418 sulfate) were from Gibco BRL (Grand Island, NY). Zeocin and LipofectAMINE™ reagent were from Invitrogen (Carlsbad, CA). Sheep erythrocytes were purchased from BioWhittaker (Walkersville, MD) and were opsonized with anti-sheep erythrocyte IgG from Cappel Organon Teknika (Durham, NC). Polyvinylidene difluoride membranes were from Schleicher and Schuell (Keene, NH).

Cell culture

COS-1 cells, stably transfected with FcγRIIA receptor cDNA, were maintained in Dulbecco's modified Eagle's medium containing 4.5 mg/ml glucose, 25 mg/ml glutamine, 100 U/ml streptomycin, 100 mg/ml penicillin, and 10% heat-inactivated fetal calf serum. COS-1 cells transfected stably with FcγRIIA were cultured in 35 mm dishes to create double expression transfectants with FcγRIIA and hCERK. The cells were transfected with 1 μg/ml pcDNA-hCERK expression vector using LipofectA-MINE Plus™ in 1 ml of opti-MEM medium at 80% confluence. One milliliter of DMEM containing 20% fetal bovine serum was added after 3 h of incubation at 37°C and 5% CO_2. To establish stable transfectants, cells were cultured with medium containing 200 μg/ml G-418 and 200 μg/ml Zeocin to select double transfectants.

Sheep erythrocytes

Sheep red blood cells were sensitized with rabbit IgG anti-sheep erythrocyte antibody as described (EIgG) (23). Phagocytosis assays were conducted as described previously (24).

hCERK expression vector

A plasmid carrying the hCERK gene was provided by Dr. Takafumi Kohama (Sankyo Co., Ltd.) (22). Construction of catalytically inactive hCERK (G198DhCERK) was done as described previously (22).

Construction of red fluorescent protein-tagged hCERK

A C-terminal fusion of human CERK and DsRed monomer was constructed by PCR amplification of hCERK and cloning into plasmid pDsRed-Monomer-N1. hCERK was amplified by PCR from the existing construct, pcDNA-hCERK, using the following primers: CERK 5′XhoI (5′-CTCGAGATGGGGCGACGGGGGCG-

3′) and CERK 3′HindIII (5′-AAGCTTGCTGTGTGAGTCTG-GCTTCG-3′). The resulting PCR product was first cloned into pCR2.1-TOPO (Invitrogen), and recombinants were subsequently digested with *Xho*I and *Hind*III to release a 1.6 kb fragment. The *Xho*I-*Hind*III CERK-containing fragment was gel-purified and ligated to pDsRed-Monomer-N1, also digested with *Xho*I and *Hind*III, creating an in-frame N-terminal fusion between CERK and the DsRed monomer. The fusion protein was tested for CERK activity and found to be biologically active.

Lipid raft isolation

Transfected COS-1 cells were fractionated as described previously (22). FcγRIIA, FcγRIIA/vector, and FcγRIIA/hCERK transfected COS-1 cells were challenged with opsonized erythrocytes (EIgG), and the EIgG not ingested were lysed. COS-1 cells were harvested by scraping them into a buffer containing 20 mM Tricine (pH 7.8), 0.25 M sucrose, and 1 mM EDTA. The cells were washed and then disrupted in the same buffer with 30 strokes in a Wheaton tissue grinder. The postnuclear supernatant fraction was obtained by centrifugation of the cell lysates at 100 *g* for 10 min. The plasma membrane fraction was removed from 30% Percoll and 0.25 M sucrose buffer after centrifugation at 84,000 *g* for 30 min. Caveolae membrane fractions were isolated from the purified plasma membrane fractions using OptiPrep gradients as described (22). Aliquots of membrane fractions and the caveolae/lipid raft fractions were analyzed by SDS-PAGE. Proteins were transferred to polyvinylidene difluoride membranes and subjected to Western blotting using anti-caveolin-1, anti-c-Myc, and anti-TRPC-1 antibodies.

Phagolysosomal fusion assay

To measure phagolysosomal fusion, cells were imaged on a Zeiss Axiovert 135 inverted microscope coupled to a cooled digital charge-coupled device camera (QImaging, Barnaby, British Columbia, Canada). Cover slips were observed using bright-field microscopy, and fluorescence was visualized using narrow band-pass discriminating filters with excitation at 535 nm and emission at 590 nm for tetramethylrhodamine. Images were obtained using Volumescan (Vaytek, Inc., Fairfield, IA) and were processed using Image-Pro Plus (Media Cybernetics, Silver Spring, MD). In some studies, mibefradil and SKF96365, inhibitors of SOCs, were used to evaluate their effect on phagocytosis and phagolysosomal fusion in the concentrations stated in each figure.

Confocal microscopy

Confocal scanning fluorescence microscopy was performed with an Olympus Fluoview FV 500. This microscope was used to obtain z series image stacks of cells. Cells were transfected with hCERK or red fluorescent protein (RFP)-tagged hCERK. Cover slips with adherent transfectants that had undergone phagocytosis were washed once with cold PBS and then fixed with 3% paraformaldehyde in PBS for 10 min at room temperature. After the first fixation, the cells were rinsed three times with PBS and permeabilized for 2 min at 25°C with 0.1% Triton X-100 in PBS. The cells were washed extensively in PBS and fixed again in 3% paraformaldehyde for 5 min. After blocking for 30 min with 3% BSA in PBS, the cells were incubated with anti-caveolin-1, anti-hCERK, or anti-TRPC-1 antibody at a dilution of 1:200 for 1 h at room temperature. Samples were washed and then labeled with the secondary FITC-conjugated rabbit anti-goat antibody (1:200 dilutions for 30 min at room temperature). To minimize nonspecific binding, 1% BSA was included in these solutions. Images from multiple confocal planes were collected.

Preparation of FITC-conjugated red blood cells

Opsonized red blood cells were incubated with 30 μg of FITC per 1×10^6 cells at room temperature for 4 h. The fluorescent conjugates were separated from unreacted fluorochromes by Sephadex G-25 column chromatography. Purified conjugates were dialyzed against PBS at pH 7.4 overnight at 4°C.

Calcium imaging

To study dynamic changes in calcium during phagocytosis, microscopy was performed using a Nikon Eclipse TE2000-U inverted microscope. To detect time-lapse changes in fluorescence in the short wavelength emission region of Indo-1, a 355HT15 exciter, a 390 LP dichroic reflector, and a 405DF43 emission filter were used. An iXon model DV8 16-bit electron multiplying charge coupled device camera cooled to −100°C (Andor Technologies, South Windsor, CT) was used.

To examine the high-speed dynamics of calcium signaling, a Perkin-Elmer FX-4400 flash lamp was used for excitation (25). This flash lamp produces pulses that are 6 μs in duration and up to 1 J in energy, which is sufficient to saturate the fluorescent labels. The excitation light is passed through a water filter to attenuate ultraviolet and infrared components ($\sim 10^9$- to 10^{10}-fold) relative to visible wavelengths. The light can be further filtered using KG-1 and interference filters before entering the epifluorescence microscope. A high-numerical aperture objective (1.45) was used to maximize sample brightness. To provide the greatest sensitivity to weak fluorescent signals, a Princeton Instruments PI-MAX2 intensified charge coupled device camera with a 5 MHz controller was used to collect images. The 1×1 K images were 2×2 binned to form the raw images shown. To reduce the amount of noise in the processed micrographs, previously described wavelet image filtration software was used before the application of a pseudocolor look-up table (26).

RESULTS

Lipid raft composition in transfectants is altered by IgG-opsonized targets and CERK expression

In a previous study (22), we used an in vitro cell culture system to evaluate the mechanism of C1P-potentiated phagocytosis. Stable transfectants of COS-1 cells expressing FcγRIIA or both FcγRIIA and hCERK were created. Those studies indicated that during FcγRIIA-mediated phagocytosis in cells overexpressing hCERK, CERK is activated and C1P is subsequently increased. Furthermore, the increase in C1P during phagocytosis led to a distinct gel-like ordered lipid phase within the cell membrane at sites of phagocytosis (22). Furthermore, cell fractionation studies revealed that hCERK was enriched in plasma membrane caveolae fractions called lipid rafts, which are signaling domains enriched in sphingolipids.

As sites of phagocytosis demonstrate physical and chemical properties of lipid rafts, the protein composition of lipid rafts with and without stimulation with EIgG was studied. Lipid rafts were obtained using cell fractionation methods, and their identity was confirmed using an anti-caveolin-1 monoclonal antibody (**Fig. 1**). As CERK and TRPC-1 have been associated with caveolin and/or lipid rafts (27–29), we speculate that TRPC-1 and its SOC-like activity may be relevant to calcium signaling in these
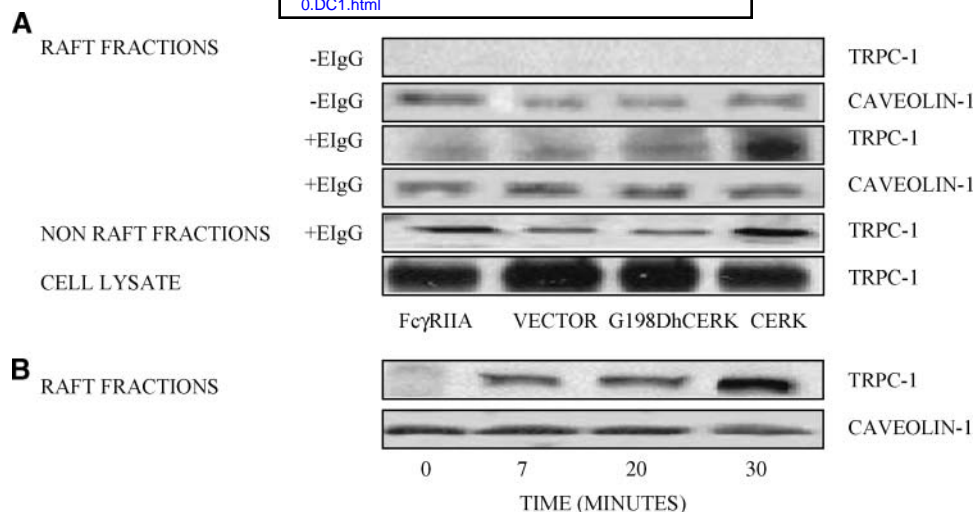
Fig. 1. Caveolin-1 and transient receptor potential channel (TRPC-1) expression in lipid rafts. Caveolin-1-containing membrane rafts were isolated as described in Methods. Samples were solubilized, and Western blots were run to detect proteins. A: TRPC-1 protein was enriched in rafts isolated from COS-1 cells overexpressing FcγRIIA, FcγRIIA/vector, FcγRIIA/hCERK, FcγRIIA/G198DhCERK, and stimulated with EIgG for 30 min. B: TRPC-1 expression in raft fractions during stimulation of FcγRIIA/hCERK transfected cells with EIgG for 7, 20, and 30 min.

transfectants. In the first series of experiments, we used an anti-TRPC-1 antibody to determine whether TRPC-1 channels are associated with lipid rafts in COS-1 transfectants. When unstimulated cells were studied, we were unable to detect TRPC-1 in lipid rafts (Fig. 1A). However, after challenging cells with EIgG, TRPC-1 was found in lipid rafts of all transfectants, although the strongest signal was found in hCERK transfected cells. TRPC-1 was also present in all nonraft fractions. Using an antibody for TRPC-1, we examined the kinetics of TRPC-1 localization to plasma membrane rafts during activation in cells transfected with hCERK (Fig. 1B). Cells were stimulated with opsonized erythrocytes (EIgG) for different periods of time and then subjected to fractionation. Western blotting revealed that TRPC-1 accumulated rapidly in raft fractions during activation but was barely detected in
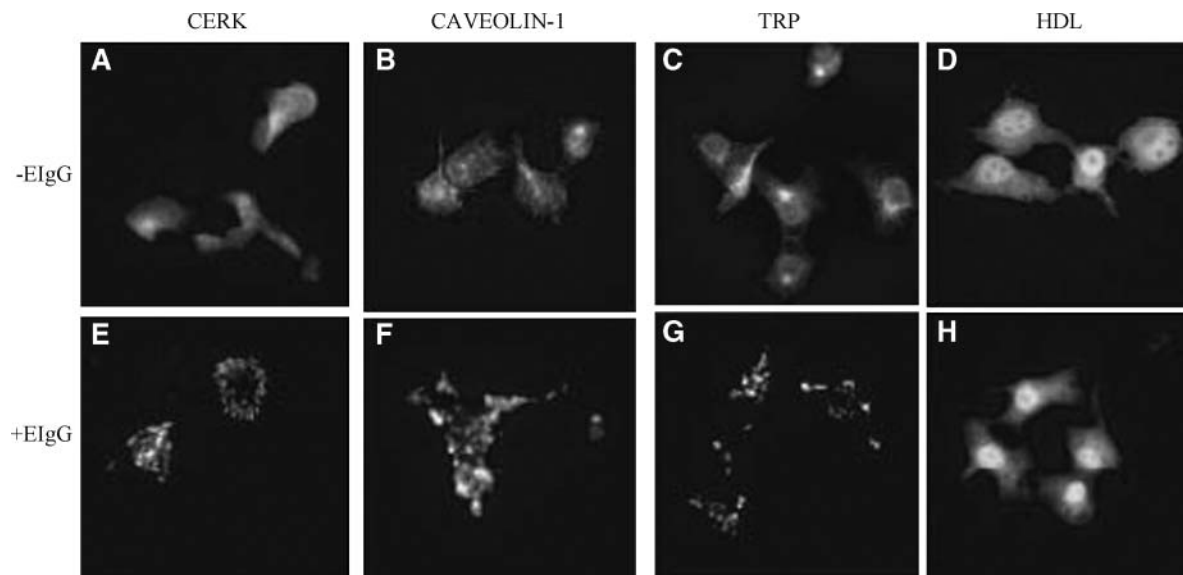

Fig. 2. Subcellular localization of human ceramide kinase (hCERK), TRPC-1, and caveolin-1 in COS-1 cells stably transfected with hCERK. COS-1 cells overexpressing hCERK were grown on cover slips and stimulated with EIgG for 30 min as described in Methods. Subcellular localization of hCERK, TRPC-1, and caveolin-1 was determined by indirect immunofluorescence using anti-hCERK, anti-TRPC-1, and anti-caveolin-1 polyclonal antibodies followed by FITC-conjugated secondary antibody and by confocal microscopy. HDL was used as a negative control. The upper panels show unstimulated cells. The lower panels show cells stimulated with EIgG for 30 min at 37°C. Cells stained with HDL were unstimulated (A–D) or stimulated with EIgG (E–H). Similar localizations were observed in five independent experiments.

rafts during resting conditions. The primary antibody was either omitted or incubated with these blocking peptides as negative controls. Similarly, hCERK also appeared rapidly in lipid rafts after stimulation (22).

Localization of caveolin-1, TRPC-1, hCERK, and HDL using immunofluorescence microscopy

To assess the cellular localization and appearance of hCERK, TRPC-1, and caveolin, confocal microscopy was performed. Unstimulated COS-1 transfectants were labeled with antibodies directed against hCERK, caveolin-1, TRPC-1, and HDL (**Fig. 2A–D**). As expected, cells were positively stained with these three reagents. When cells were incubated with EIgG for 30 min at 37°C, hCERK, caveolin-1, and TRPC-1 were redistributed at the cell surface (Fig. 2E–H). Cells labeled with HDL were used as negative controls; HDL did not redistribute

after incubation with EIgG (Fig. 2H). Exposure to EIgG caused a more punctate appearance of these markers.

To monitor the subcellular localization of hCERK during phagocytosis, RFP-tagged hCERK was used. When EIgG conjugated directly with FITC was incubated with COS-1 cells transiently transfected with RFP-hCERK for 30 min at 37°C, we observed that FITC-conjugated red blood cells and RFP-hCERK colocalized during phagocytosis (**Fig. 3A**).

Cells transiently transfected with RFP-hCERK were incubated with EIgG for 30 min at 37°C. After lysis of uningested EIgG, cells were fixed and then labeled with anti-caveolin-1. Samples were washed and then labeled with the secondary FITC-conjugated rabbit anti-goat antibody. Optical images of CERK revealed the colocalization of hCERK and caveolin-1 (Fig. 3B). Coimmunoprecipitation or colocalization of caveolins with TRPC-1 and TRPC-3 have been reported previously (29, 30).
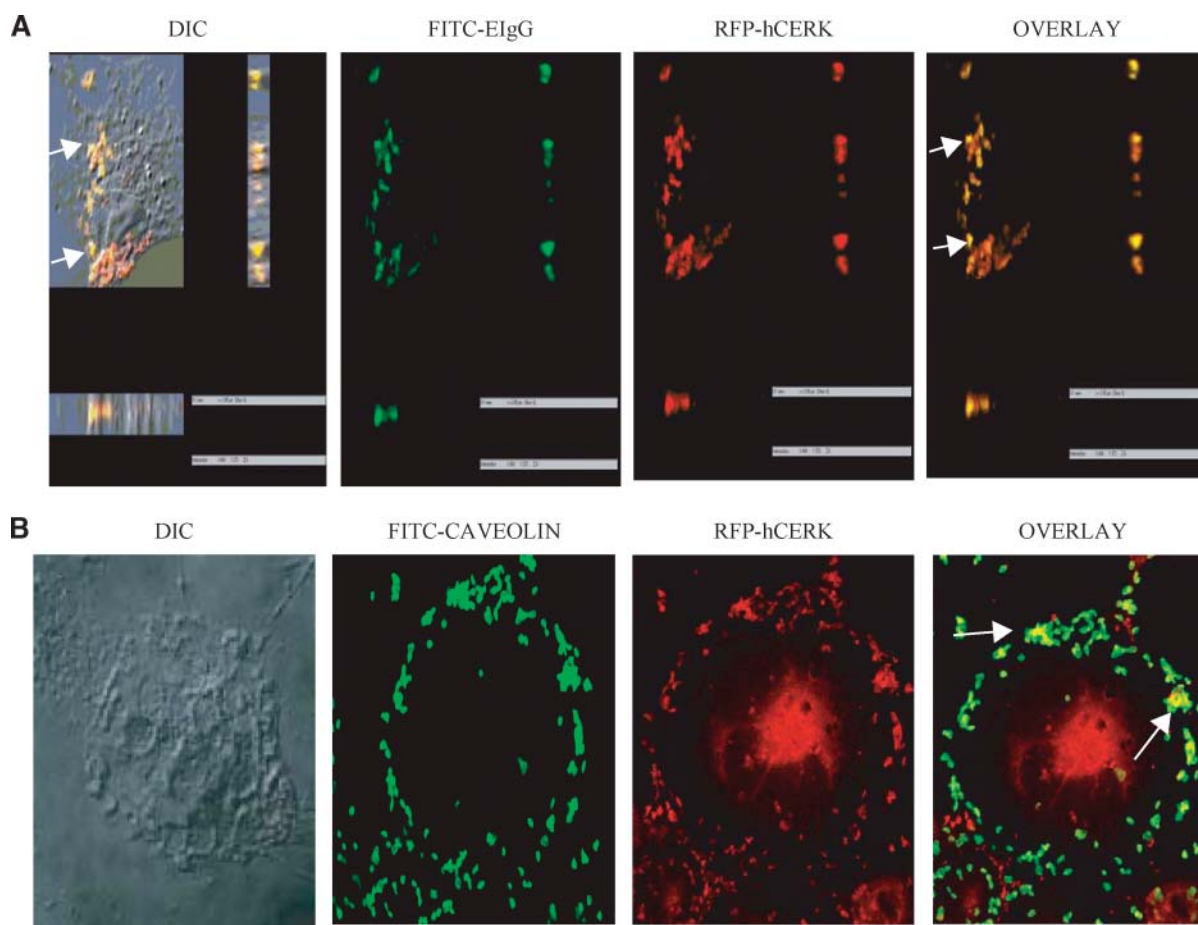

Fig. 3. A: Colocalization of red fluorescent protein-hCERK (RFP-hCERK) and FITC-conjugated EIgG. COS-1 cells bearing FcγRIIA were transiently transfected with RFP-tagged hCERK and stimulated with EIgG for 30 min at 37°C as described in Methods. After phagocytosis, bound but not internalized red blood cells were lysed, followed by microscope observations to detect the colocalization of hCERK and targets. Stacks of fluorescence micrographs were obtained from individual cells followed by deconvolution analyses of the z-scans. The first panel displays the colocalization of hCERK and EIgG together in a differential interference contrast (DIC) image (arrows). The second panel displays the FITC image. The third panel shows RFP-hCERK fluorescence. The last panel shows an overlay of the second and third panels. B: Colocalization of RFP-hCERK and caveolin-1 in transiently transfected COS-1 cells. COS-1 cells were transiently transfected with RFP-tagged hCERK and stimulated with EIgG for 30 min at 37°C as described in Methods. After phagocytosis, exes of noninternalized red blood cells were lysed. Subcellular colocalization of hCERK and caveolin-1 was determined by indirect immunofluorescence using secondary anti-rabbit IgG FITC-conjugated antibody developed in goat and by confocal microscopy (arrows). The first panel displays DIC image, the second panel displays FITC image, the third panel shows RFP-hCERK, and the last panel shows an overlay of second and third panels.

Time-lapse calcium signaling experiments

To measure phagocytosis-induced Ca^{2+} signaling, COS-1 cells stably transfected with hCERK were labeled with Indo-1 as described in Methods. Cells were placed on the microscope and EIgGs were added. The first image was acquired at time zero, and images were subsequently taken every 4 min for 3 h. **Figure 4** illustrates the Indo-1 intensity over this period of time. To minimize photochemical damage, the light was shuttered between exposures. FcγRIIA transfected control cells and FcγRIIA/hCERK transfected cells were compared. As these kinetic studies indicate, phagocytosis-induced Ca^{2+} levels in COS-1 hCERK transfected cells were significantly higher than those in FcγRIIA transfected cells. This supports a role for CERK in phagocytosis-associated intracellular signaling.

Observation of quantal calcium release events

To further illuminate the contribution of CERK to phagosomal Ca^{2+} signaling, high-speed microscopy was used. One advantage of this approach is that the image is acquired in a period of time that is substantially less than the gating time of membrane channels; thus, multiple gating cycles cannot contribute to the image. Furthermore, large numbers of channels are not likely to be simultaneously engaged during image acquisition. Finally, significant diffusion of the Ca^{2+}/probe complex is not possible during exposure. As described in Methods, fluorescent samples were exposed to a flash of excitation light. To establish this procedure, we examined fluorescent beads. **Figure 5A–F** shows data concerning blue fluorescent beads; these data were obtained using the same excitation/emission filters and excitation flash as those used below for cells. When the beads were exposed to a single 6 μs flash, the fluorescence image in Fig. 5B was obtained. This image, as well as many other bead images, suggests that the illumination field provided by the flash lamp was acceptable. As the cell data below use wavelet filtration for noise removal, this image of fluorescence beads was processed using this software. Because of its many advantages, such as the ability to remove uncorrelated noise, wavelet software is an important emerging technology (31, 32). Wavelet transformation of the single frame in Fig. 5B returned a very similar but somewhat sharper image (Fig. 5C). As the image was very clean, little noise was removed (Fig. 5D). When image stacks of 100 frames of the raw or wavelet-filtered images were summed, essentially the same images were again returned (Fig. 5E, F, respectively). Hence, these studies with dim fluorescent beads confirmed that the hardware and software components were working as predicted.

Using this approach, we first examined Ca^{2+} signaling in transfectants expressing only FcγRIIA during phagocytosis. Although the region of the cell in Fig. 5H appears brighter than the surrounding area, wavelet filtration did not produce a convincing signal within the cell in general or at the phagosomes in particular. When a series of 500 high-speed images of this same cell were collapsed into a single image (Fig. 5K), no significant signal was observed.
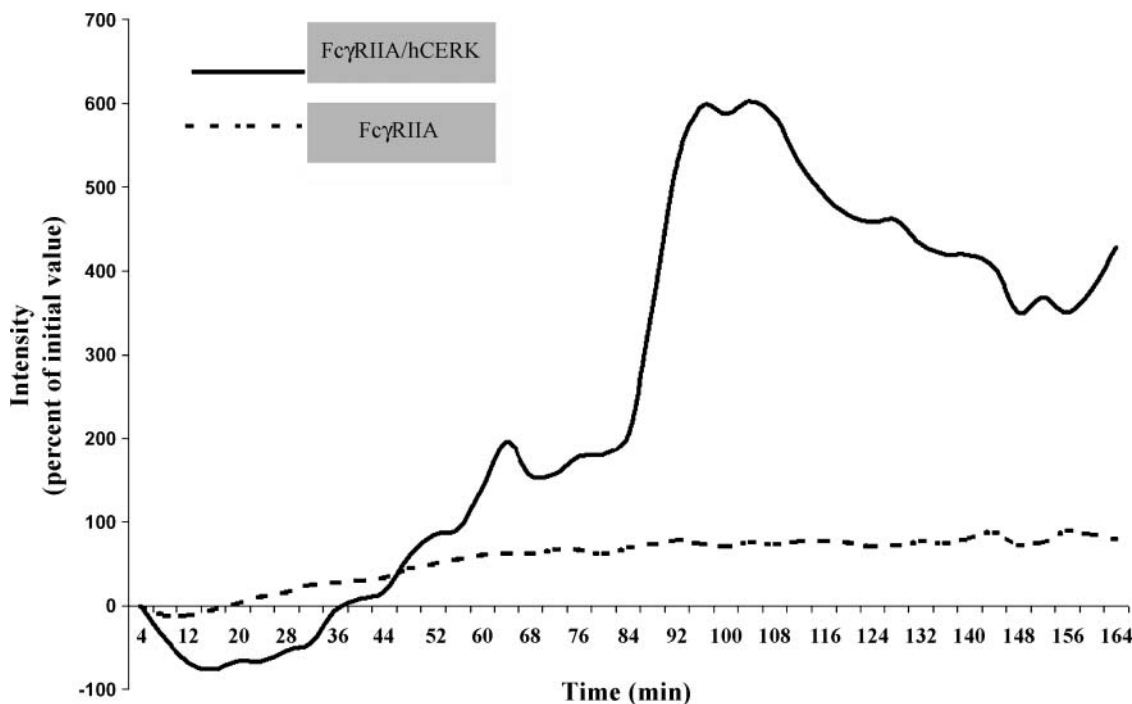

Fig. 4. Time-lapse measurements of Indo-1 intensity during interaction with EIgG in COS-1 cells. COS-1 cells were labeled with Indo-1 as described in Methods. The cells were placed on a microscope slide, followed by the addition of EIgG. The intensity was recorded as a function of time. FcγRIIA transfected cells showed a minimal response (n = 3; all three showed the same range of Ca^{2+} signal) (dashed line). FcγRIIA/hCERK transfected cells (n = 5; 60% of the cells showed increased Ca^{2+} signal; $P < 0.001$) (solid line) showed a much more robust response.

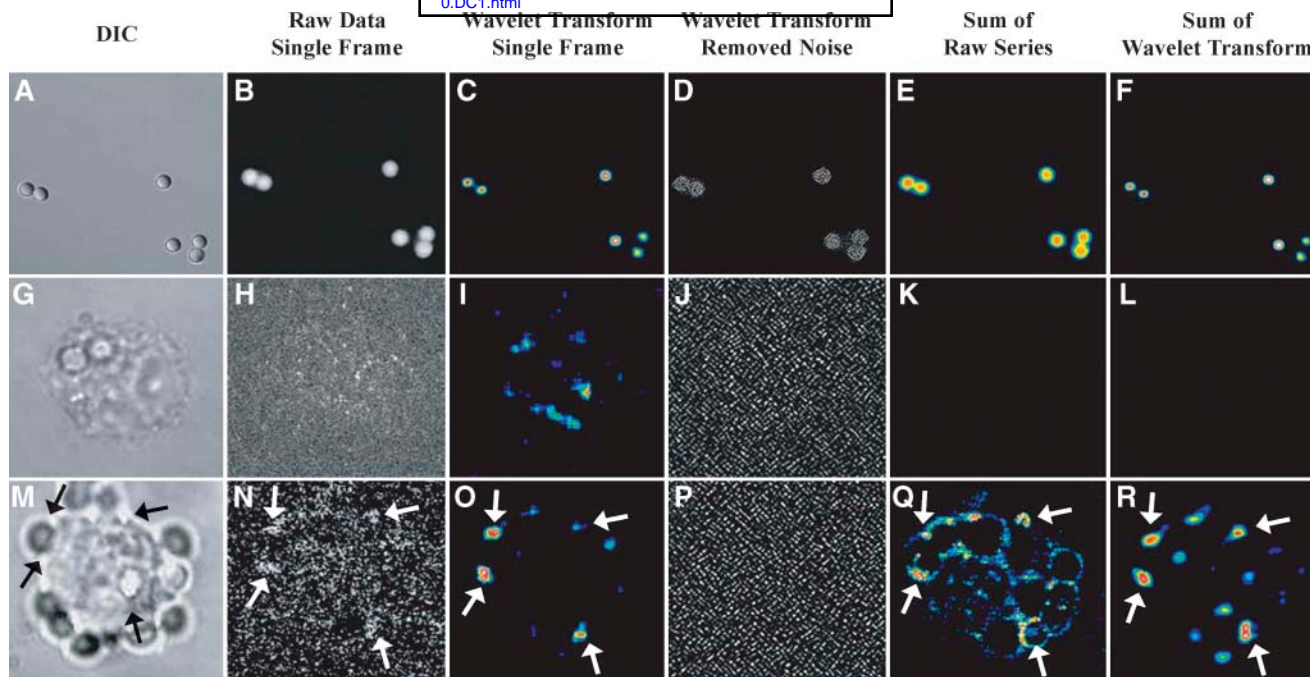| DIC	Raw Data Single Frame	Wavelet Transform Single Frame	Wavelet Transform Removed Noise	Sum of Raw Series	Sum of Wavelet Transform

Fig. 5. Analyses of high-speed images. Differential interference contrast (DIC; column 1, A, G, M) and fluorescence images (columns 2 through 6) are shown. A–F show a series of experiments using blue fluorescent beads. A single exposure of the flash-lamp yielded a high-quality image of the beads (B). A wavelet transform of this image returned essentially this same image (wavelet coefficient = 18; a multicolor look up table was used for display purposes). The result using a wavelet coefficient of 1 is shown in D. When 100 frames of a high-speed series were summed, the raw data and the wavelet-filtered data yielded matching results. Transfectants expressing only FcγRIIA did not yield a definitive fluorescence signal (G–L). However, transfectants expressing FcγRIIA and CERK displayed a signal near pseudopods and phagosomes. Dim structures are noted in N. Regions with noted repetitions throughout the sequence of 500 images are indicated with arrows. Wavelet filtration indicated two particularly strong signals near the same target (wavelet coefficient = 16) (O). Much of the noise removed from the image is shown in P, which used a wavelet coefficient of 2. When the raw data of all 500 images were summed, the image in Q was obtained. This shows that the wavelet-filtered frame is a subset of the raw image sum. The wavelet sum shows the primary area of signal activity (R). These data indicate that CERK transfection leads to punctate regions of signaling near targets. Arrows indicate Ca release sites.

(To allow proper comparisons, the gain and offset of panel K were the same as those of panel Q, and those of panel L matched panel R.) Similar results were obtained when the wavelet-filtered images were collapsed into a single frame (Fig. 5L). Hence, the FcγRIIA-mediated phagocytosis of EIgG by these transfectants did not trigger an apparent calcium signal. Our catalytic inactive mutant FcγRIIA/ G198DhCERK does not have any signal under identical conditions (data not shown).

We next explored the contribution of hCERK expression to Ca²⁺ signaling in transfectants during phagocytosis. The beginning of this experiment corresponded to roughly 50 min after EIgGs were first added to the sample (as indicated in the separate study in Fig. 4). As indicated in the raw data of Fig. 5N, two periphagosomal calcium signals were noted in this frame. Wavelet filtration of the data was performed to minimize the contribution of noise to this image. After this procedure was performed, these same two regions were quite apparent in the filtered image (Fig. 5O). A substantial component of the uncorrelated noise removed from the original raw image is shown in Fig. 5P. To confirm that the wavelet-filtered single frame of Fig. 5O was contained in the summed (long time scale) image, the 500 raw images were collapsed into a single frame (Fig. 5Q) and then compared with the filtered

single frame (Fig. 5O). Indeed, both robust signals reported by the wavelet filtration protocol as well as areas of marginal intensity are represented in the collapsed raw image. When the 500 wavelet-filtered images were collapsed onto a single frame, all of the significant signaling areas represented in the summed raw data (Fig. 5Q) were represented in the summed wavelet-filtered image (Fig. 5R). The slight loss in apparent resolution was more than offset by the dramatic reduction in noise. Hence, CERK expression in combination with FcγRIIA promotes punctate Ca²⁺ signaling events at phagosomes or phagocytic cups.

As alluded to above, one of the key advantages of this imaging approach is that multiple images of the same cell can be acquired in rapid succession without frame averaging. To observe the underlying kinetic behavior of the CERK-induced signaling events, 19 consecutive frames acquired at 10 Hz extracted from the series are shown in **Fig. 6**. To provide a reference, Fig. 6, frame 1, shows an image of the cell with the frequent sites of signals shown as red dots. Frames 2 through 20 illustrate the time-dependent quantal release of Ca²⁺ at sites of EIgG contact or phagocytosis. These Ca²⁺ sites flicker during observations and are only observed at several sites throughout the cell in which EIgGs are located. Furthermore, it would
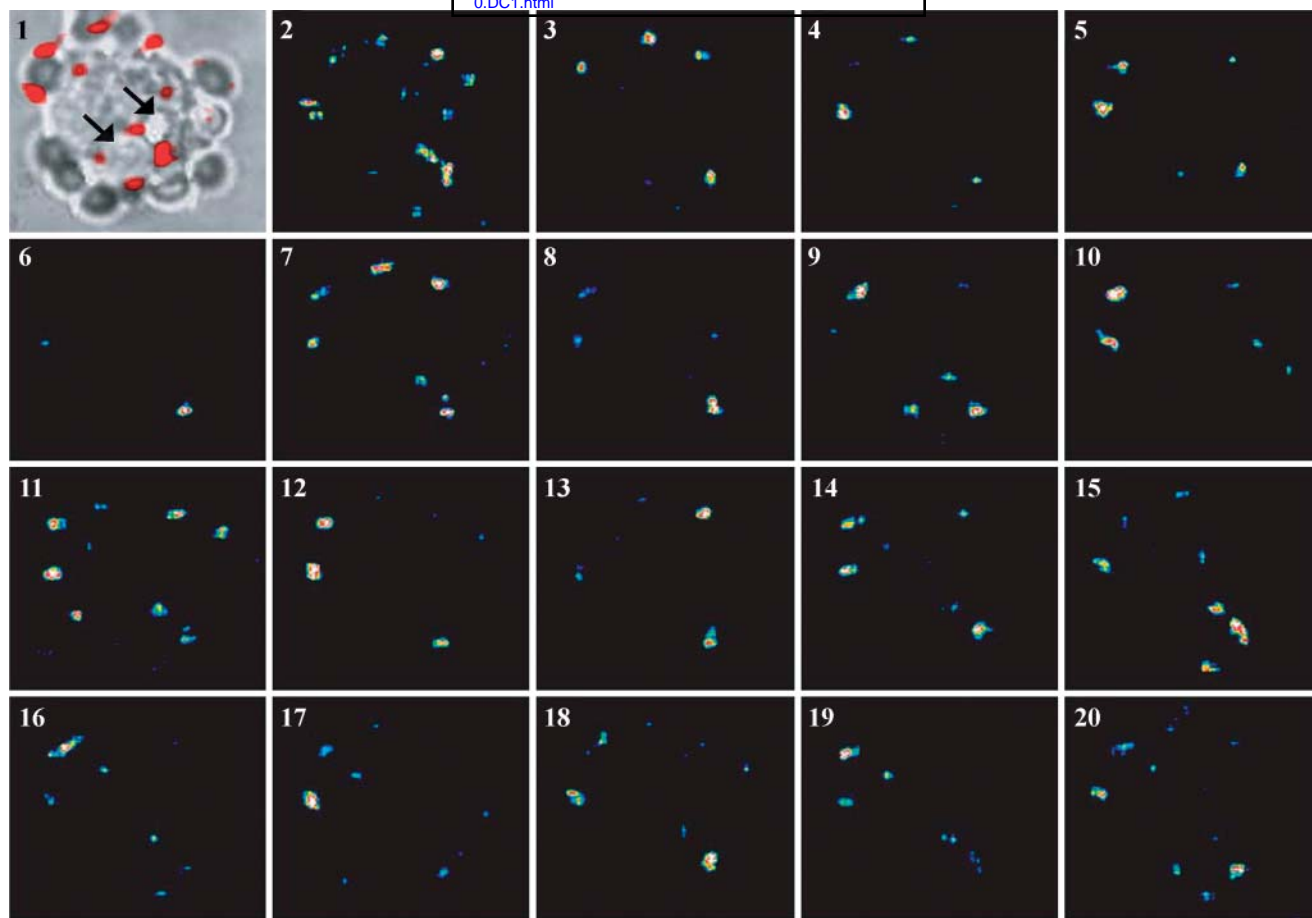
Fig. 6. Spatiotemporal properties of Ca^{2+} signals during stimulation with EIgG. Transfectants expressing FcγRIIA and CERK were labeled with Indo-1, followed by incubation with EIgG. Micrographs of Indo-1-labeled cells were acquired using an illumination exposure time of 6 μs, and the readout between frames was 100 ms. Frame 1 shows a micrograph with the principal signaling regions labeled red. Arrows indidcate phagocytic targets and punctate Ca signaling events. Frames 2–20 show 19 consecutive images of Ca^{2+} signals, which are restricted to pseudopods and periphagosomal regions. Specific regions of signals repeated over time but were asynchronous with other signals in the cell.

seem that Ca^{2+} signaling in the vicinity of one EIgG is not correlated with that at distant sites, which implies that some generalized event, such as membrane depolarization, is not mediating the response. However, one spatial site of Ca^{2+} release could be triggered multiple times during the observations (see supplementary movie). This suggests that the essential components of the Ca^{2+} signaling apparatus are not rapidly moving through the cell. Thus, CERK expression by transfectants promotes rapid, localized Ca^{2+} signaling events during phagocytosis.

hCERK transfection of COS-1 cells increases phagolysosomal fusion

Phagolysosome fusion is a highly regulated event that is essential for the intracellular killing of microorganisms. Calcium is a key messenger in many cell functions, including phagosome-to-lysosome fusion (33). The question of whether the transfection of COS-1 cells with FcγRIIA/hCERK increases phagolysosome formation compared with cells bearing only FcγRIIA, FcγRIIA/vector, or FcγRIIA/G198DhCERK was studied. Adherent cells were allowed to internalize EIgG for 30 min at 37°C. External EIgGs were removed by hypotonic lysis. Cells were then labeled with LysoTracker Red DND-99 at 37°C and imaged as described in Methods. The scoring system used is shown for hCERK transfected cells with internalized EIgG. When cells were labeled with LysoTracker, phagosomes that fused with lysosomes displayed a bright ring on their perimeter, whereas phagosomes that did not undergo fusion did not. The percentage of phagolysosome fusion was compared by cell line (**Fig. 7**). hCERK transfected cells had a mean rate of fusion of 90%, G198DhCERK cells had a mean rate of 76% ($P < 0.02$), FcγRIIA transfected cells had a mean rate of 65% ($P < 0.001$), and cells transfected with the empty vector had a mean rate of 70% ($P < 0.001$). There is no statistically significant difference in the level of phagolysomal fusion between control cells and inactive CERK. However, there is a significant difference between the values for inactive CERK and hCERK.

Pharmacological characterization of phagocytosis and phagolysosomal fusion

Our previous studies indicated that during the activation of COS-1 cells by EIgG in the presence of hCERK, C1P increases significantly (22). The changes in Ca^{2+} signaling are not likely to be mediated directly by CERK but rather
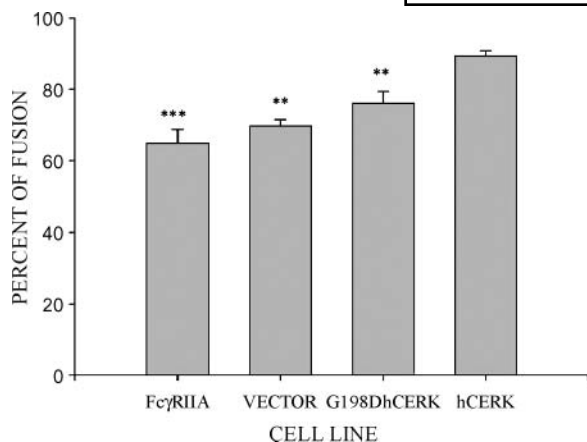
Fig. 7. Phagolysosome fusion in cells overexpressing FcγRIIA, FcγRIIA/vector, FcγRIIA/hCERK, and FcγRIIA/G198DhCERK. Cells bearing hCERK have increased levels of phagosome-lysosome fusion compared with cells bearing only FcγRIIA, FcγRIIA/vector, and FcγRIIA/G198DhCERK. Adherent cells were allowed to internalize EIgG. External EIgGs were removed by hypotonic lysis. Cells were then labeled with LysoTracker Red DND-99 at 20 μM in PBS for 5 min at $37°C$ and imaged as described in Methods. The percentage of phagolysosome fusion by each cell line is shown (n = 3). hCERK-bearing cells had a mean rate of fusion of 90%, G198DhCERK cells had a mean rate of 76% ($P < 0.02$), FcγRIIA transfected cells had a mean rate of 65% ($P < 0.001$), and cells transfected with the empty vector had a mean rate of 70% ($P < 0.001$). There was no statistically significant difference in the level of phagolysomal fusion between control cells and inactive CERK. However, there was a statistically significant difference between the values for inactive CERK and hCERK. Error bars indicate $\pm$ SD. ** $P < 0.02$, *** $P < 0.001$.

should require the participation of Ca^{2+} channels. As TRPC-1 colocalizes with CERK and TRP channels are potential candidates for SOC channel activity (34), we examined the effect of pharmacologic agents directed against this class of molecules. One such agent is the econazole derivative SKF96365, which blocks SOCs in the low- to mid-micromolar range. Another pharmacologic reagent is the SOC inhibitor CAI. COS-1 cells were challenged with EIgG at $37°C$ for 30 min. The Ca^{2+} channel inhibitors SKF96365 (15 μM), CAI (20–30 μM), and $CdCl_2$ (3–15 μM) significantly decreased the ability of COS-1 cells transfected with hCERK to undergo Fc-mediated phagocytosis (**Fig. 8A–C**). SKF96365 (15 μM) decreased the phagocytic index of hCERK transfectants by 20% compared with the control. Under these conditions, no changes in the phagocytic index were seen when FcγRIIA or G198DhCERK transfectants were treated with 5–30 μM SKF96365 or CAI (Fig. 8A, B). Thus, pharmacological blockade with these three reagents diminished phagocytosis in hCERK transfected cells. When hCERK transfected cells were treated with SKF96365, phagolysosomal fusion was diminished significantly by 20% (Fig. 8D). Untreated hCERK transfectants had a mean rate of fusion of 90%, cells treated with 15 μM SKF96365 had a mean rate of 73% ($P < 0.02$), and cells treated with 50 μM SKF96365 had a mean rate of 69% ($P < 0.02$). These data suggest that the enhancing effects of CERK expression on

phagolysosome formation require the participation of Ca^{2+} channels.

DISCUSSION

We have shown previously that in neutrophils, C1P is formed by a calcium-dependent CERK located in the plasma membrane during IgG-dependent phagocytosis (35). To better understand CERK's potential role in Fc receptor function, transfectants that expressed both FcγRIIA and hCERK were prepared (22). These transfectants displayed enhanced CERK activity and C1P generation during Fc receptor-mediated phagocytosis (22). Using COS-1 cells stably transfected with FcγRIIA and hCERK, we show that the activation of CERK with concomitant accumulation of C1P altered Ca^{2+} signaling near the phagosome and significantly promoted neutrophil phagocytosis and phagolysosomal formation (35).

Previous studies have shown that phagocytosis is accompanied by Ca^{2+} signaling at pseudopods and the periphagosomal region (36–38). In comparing the panels of Fig. 6M–R, both pseudopodial and periphagosomal Ca^{2+} signaling were observed in COS-1 cells expressing FcγRIIA and hCERK. However, in contrast to those previous studies that reported a uniform distribution of Ca^{2+} at these sites, our studies using very brief excitation exposures show a punctate distribution of Ca^{2+} release at pseudopods and in the periphagosomal vicinity. When the raw images are summed over 500 frames, the resulting image resembles those obtained in experiments using longer exposure times. However, high-speed imaging indicates that Ca^{2+} signaling in this model system occurs at hot spots that represent brief, but intense, Ca^{2+} release events. These sites of enhanced Ca^{2+} signaling are not random but repeat at the same spatial location quite often. These Ca^{2+} signaling hot spots exist for periods of time (<100 ms) that are not inconsistent with channel-gating times. These quantal release events may correspond to a relatively small number of ion channel-opening events. The more uniform distributions observed in other studies may be attributable to the facts that the high-speed technique used here minimizes the diffusion of the probe and ion during the exposure and that the relatively high local concentration saturates nearby calcium probes at release sites that are sufficiently bright to be detected. Alternatively, there may be cell-to-cell differences between leukocytes and COS-1 transfectants that account for these differences. For example, monocytes and neutrophils might express many more Ca^{2+} release sites near phagosomes that create a uniform appearance during imaging. Hence, the localized and asynchronous phagosome-associated Ca^{2+} signals reported above should be regarded as the CERK-related component of COS-1 transfectant signaling, not necessarily as a complete reconstitution of the phagocytosis-associated signaling pathway.

Lipid rafts are thought to be loci of signal transduction, including Ca^{2+} signaling (39). CERK binds to calmodulin (40) as well as accumulates in lipid rafts during Fc
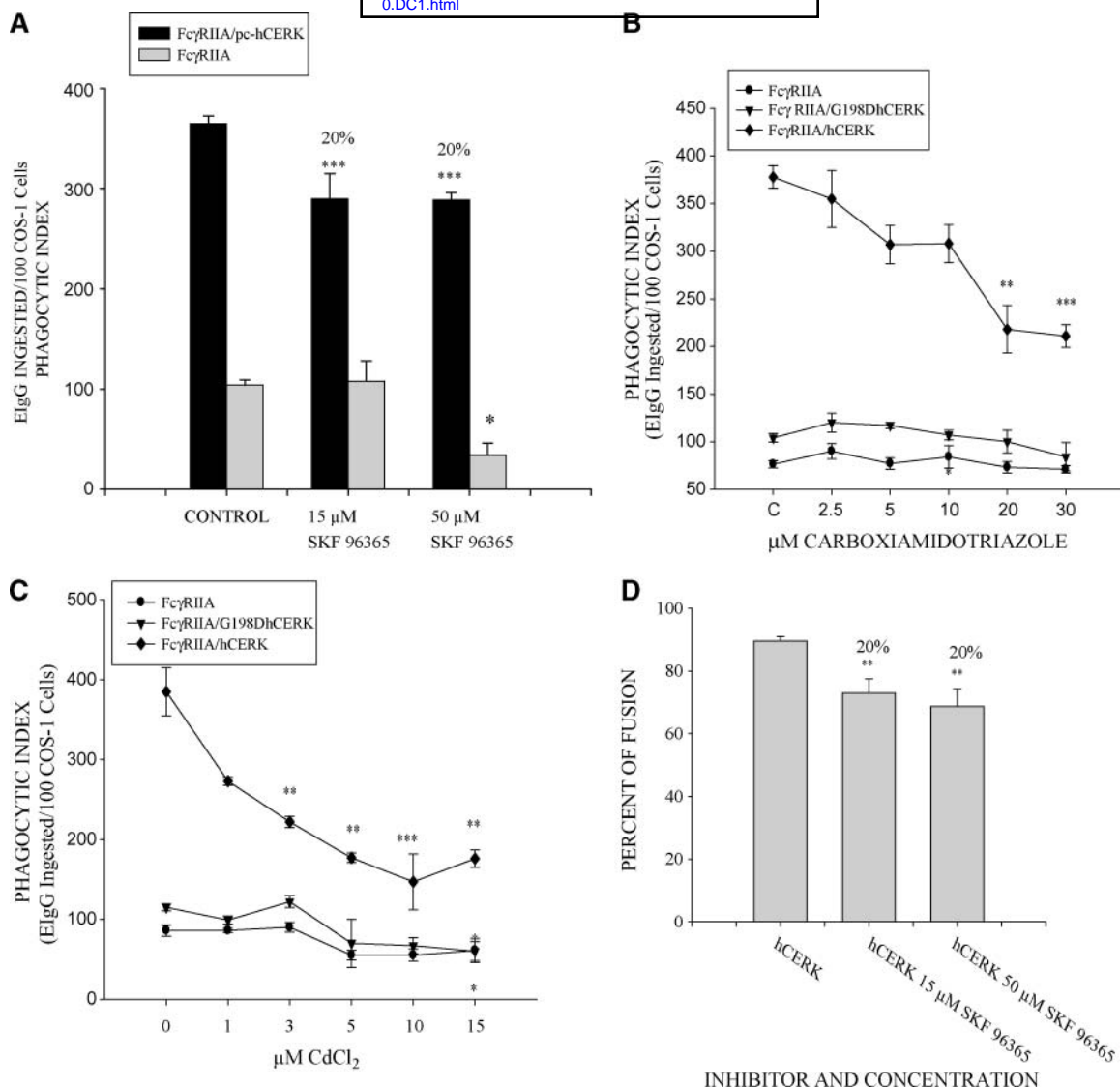
Fig. 8. Effect of channel inhibitors on phagocytic index and phagolysosomal fusion. COS-1 cells (4×10^6/dish) expressing FcγRIIA, FcγRIIA/hCERK, and FcγRIIA/G198DhCERK were pretreated for 20 min with inhibitors at the concentrations listed. Cells were challenged with EIgG (1×10^9/ml) in phosphate-buffered saline containing the inhibitor. At the 30 min time point, cells were removed with trypsin. The EIgGs not internalized were removed by lysis, and the phagocytic index was determined as described in Methods. A: Concentration of 15–50 μM SKF96365. B: Concentration of 2.5–30 μM carboxyamidazole. C: Concentration of 0–15 μM CdCl₂. D: Quantitative data involving the percentage of phagolysosome fusion in hCERK transfected cells in the presence of SKF96365. Values represent means ± SD of three experiments. * $P < 0.5$, ** $P < 0.02$, *** $P < 0.001$, difference between hCERK transfected cells treated with the inhibitor compared with untreated cells. Untreated hCERK transfectants had a mean rate of fusion of 90%, cells treated with 15 μM SKF96365 had a mean rate of 73% ($P < 0.02$), and cells treated with 50 μM SKF96365 had a mean rate of 69% ($P < 0.02$).

receptor-mediated phagocytosis (22). Although CERK may participate in Ca^{2+} signaling, it does not directly mediate Ca^{2+} movement across cellular membranes. Therefore, we speculated that a Ca^{2+} signaling conduit exists that is influenced by CERK. As other studies have demonstrated that TRPC-1 interacts with caveolin (28, 29), we examined the intracellular trafficking of CERK and TRPC-1. Our experiments show that CERK and TRPC-1 colocalize to lipid rafts, as judged by cell fractionation during Fc receptor-mediated phagocytosis. Using fluorescence microscopy, we showed that CERK and TRPC-1 colocalize to the same regions of the cell. Furthermore, fluorescence microscopy has also shown that RFP-hCERK

and FITC-conjugated EIgG colocalized during phagocytosis. Although we have not demonstrated causality, our studies do suggest that TRPC-1 is a leading candidate for a potential signaling partner relevant to CERK.

Members of the TRP family of gene products, especially TRPC-1, have been tentatively associated with the physiological role of SOC activity (41). Several plasma membrane TRPC proteins interact with intracellular inositol 3-phosphate receptors, suggesting that they communicate with Ca^{2+} stores (42), whereas others are apparently independent of Ca^{2+} stores (43). Using pharmacological probes that influence the activity of SOC, we found that these drugs diminish phagocytosis and phagolysosomal

fusion in hCERK transfectants. Specifically, the Ca^{2+} channel blockers $CdCl_2$, CAI, and SKF93365 significantly decreased the ability of COS-1 cells transfected with hCERK to undergo Fc-mediated phagocytosis and phagolysosomal fusion. At the concentrations used in these studies, these agents did not affect activated CERK activity compared with control cells (data not shown). Although the imaging studies provided structural evidence for the colocalization of TRPC-1 and CERK, these findings are consistent with the idea that SOC activity, possibly mediated by TRP channels, are participants in phagocyte function. This suggestion is consistent with previous findings that exogenously added C1P enhances store-operated Ca^{2+} entry (17) and that SOCs participate in phagocyte function in vitro and in vivo (44, 45).

The present study has also shown that CERK enhances phagolysosome formation. This finding is consistent with the observation that CERK-mediated C1P production participates in mast cell degranulation (46), which represents another Ca^{2+}-driven membrane fusion event. Transfectants expressing a catalytically inactive form of the CERK gene demonstrated reduced phagolysosome formation (Fig. 8). SOC blockers also reduced phagolysosome formation to a similar extent (Fig. 8). This finding is in general agreement with previous work suggesting that Ca^{2+} participates in phagolysosome formation.

We used a previously established in vitro system that has the ability to recapitulate and potentiate a phagocytic response in an otherwise nonphagocytic cell and that provides a unique model system for the discovery of new components of the phagocytic response. Our data suggest a speculative model of signal transduction in this transfectant system. EIgG-mediated ligation of FcγRIIA leads to the accumulation of CERK and TRPC-1 at lipid rafts, which are key participants in signal transduction. The CERK activity doubled in the raft fraction at 7 min and tripled at 30 min after stimulation (22). Ceramide generation from sphingomyelin occurs primarily in lipid rafts (47), where it may facilitate the clustering of FcγRIIA in rafts (48). In parallel, TRPC-1 accumulated in lipid rafts. Although optical microscopy is insufficient to prove that TRPC-1 and CERK occupy the same rafts, their copurification and extensive colocalization support this idea. Ca^{2+} signaling is one function associated with lipid rafts. The quantal Ca^{2+} bursts seen in the present study at pseudopods and phagosome membranes may represent Ca^{2+} release at local regions of signaling. These signals promote the increases in phagocytosis and phagolysosome fusion. jlr

REFERENCES

1. Jones, S., F. P. Lindberg, and E. J. Brown. (1999) Phagocytosis. *In* Fundamental Immunology. Vol. 1. W. E. Paul, editor. Lippincott-Raven, Philadelphia, PA. 997–1020.

2. Ravetch, J., and S. Bolland. 2001. IgG Fc receptors. *Annu. Rev. Immunol.* **19:** 275–290.

3. Brown, E. 1992. Complement receptors, adhesions, and phagocytosis. *Infect. Agents Dis.* **1:** 63–70.

4. Beron, W., C. Alvarez-Dominquez, L. Mayorga, and P. D. Stahl. 1995. Membrane trafficking along the phagocytic pathway. *Trends Cell Biol.* **5:** 100–104.

5. Burgoyne, R., and M. J. Geisow. 1989. The annexin family of calcium-binding proteins. *Cell Calcium.* **10:** 1–10.

6. Borregard, N., and L. A. Boxer. (2005) Disorders of neutrophil function. In Williams Hematology, 7th edition. M. Lichtman, E. Beutler, T. J. Kipps, V. Seligsohn, K. Kaushansky, and J. T. Prchal, editors. McGraw-Hill, New York. 921–957.

7. Mellström, B., and R. Naranjo. 2001. Ca^{2+}-dependent transcriptional repression and derepression: DREAM, a direct effector. *Semin. Cell Dev. Biol.* **12:** 59–63.

8. Hofmann, T., G. Obukhov, M. Schaefer, C. Harteneck, T. Gudermann, and G. Schultz. 1999. Direct activation of TRPC-6 and TRPC-3 channels by diacylglycerol. *Nature.* **397:** 259–263.

9. Mignen, O., and T. Shuttleworth. 2000. I_{ARC}, a novel arachidonate-regulated, noncapacitative Ca^{2+} entry channel. *J. Biol. Chem.* **275:** 9114–9119.

10. Boulay, G., M. Brown, N. Qin, M. Jiang, A. Dietrich, M. X. Zhu, Z. Chen, M. Birnbaumer, K. Mikoshiba, and L. Birnbaumer. 1999. Modulation of Ca^{2+} entry by polypeptides of the inositol 1,4,5-triphosphate receptor (IP3R) that bind transient receptor potential (TRP): evidence for the roles of TRP and IP3R in store depletion activated Ca^{2+} entry. *Proc. Natl. Acad. Sci. USA.* **96:** 14955–14960.

11. Spiegel, S., and S. Milstein. 2002. Sphingosine-1-phosphate, a key signaling molecule. *J. Biol. Chem.* **277:** 25851–25854.

12. Mayer zu Heringdort, D., C. J. van Koppen, and K. H. Jacobs. 1997. Molecular diversity of sphingolipid signaling. *FEBS Lett.* **410:** 34–38.

13. Xu, Y., K. Zhu, G. Hong, W. Wu, L. M. Baudthuin, Y. Xiao, and D. C. Damron. 2000. Sphingosylphosphorylcholine is a ligand for ovarian cancer G-protein-coupled receptor 1. *Nat. Cell Biol.* **2:** 261–267.

14. Gomez-Munoz, A., J. Y. Kong, B. Salh, and U. P. Steinbrecher. 2004. Ceramide-1-phosphate blocks apoptosis through inhibition of acid sphingomyelinase in macrophages. *J. Lipid Res.* **45:** 99–105.

15. Pettus, B., A. Bielawska, P. Subramanian, D. S. Wijesinghe, M. Maceyka, C. C. Leslie, J. H. Evans, J. Freiberg, P. Roddy, Y. A. Hannun, et al. 2004. Ceramide 1-phosphate is a direct activator of cytosolic phospholipase A2. *J. Biol. Chem.* **279:** 11320–11326.

16. Gomez-Munoz, A., D. W. Waggoner, L. O'Brien, and D. N. Brindley. 1995. Interaction of ceramides, sphingosine, and sphingosine 1-phosphate in regulating DNA synthesis and phospholipase D activity. *J. Biol. Chem.* **270:** 26318–26325.

17. Törnquist, K., C. Ramström, B. Rudnäs, K. Klika, B. Dugué, J. Adams, R. Zipkin, K. Pihlaja, and M. Pasternack. 2002. Ceramide 1-(2-cyanoethyl) phosphate enhances store-operated Ca^{2+} entry in thyroid FRTL-5 cells. *Eur. J. Biochem.* **253:** 1–11.

18. Gomez-Munoz, A., P. A. Duffy, A. Martin, L. O'Brien, H. S. Byun, R. Bittman, and D. N. Brindley. 1995. Short-chain ceramide-1-phosphates are novel stimulators of DNA synthesis and cell division: antagonism by cell-permeable ceramides. *Mol. Pharmacol.* **47:** 833–899.

19. Gomez-Munoz, A., L. M. Frago, L. Alvarez, and I. Varela-Nieto. 1997. Stimulation of DNA synthesis by natural ceramide 1-phosphate. *Biochem. J.* **325:** 435–440.

20. Rile, G., Y. Yatomi, T. Takafuta, and Y. Ozaki. 2003. Ceramide 1-phosphate formation in neutrophils. *Acta Haematol.* **109:** 76–83.

21. Gijsbers, S., G. P. Mannaerts, B. Himpens, and P. P. Van Veldhoven. 1999. N-Acetyl-sphingenine-1-phosphate is a potent calcium mobilizing agent. *FEBS Lett.* **453:** 269–272.

22. Hinkovska-Galcheva, V., L. Boxer, A. Kindzelcki, M. Hiraoka, A. Abe, H. R. Petty, and J. A. Shayman. 2005. Ceramide-1-phosphate: a mediator of phagocytosis. *J. Biol. Chem.* **280:** 26612–26621.

23. Suchard, S., V. Hinkovska-Galcheva, P. Mansfield, L. Boxer, and J. Shayman. 1997. Ceramide inhibits IgG-dependent phagocytosis in human polymorphonuclear leukocytes. *Blood.* **89:** 2139–2147.

24. Hinkovska-Galcheva, V., L. Kjeldsen, P. Mansfield, L. Boxer, J. A. Shayman, and S. Suchard. 1998. Activation of a plasma membrane-associated neutral sphingomyelinase and concomitant ceramide accumulation during IgG-dependent phagocytosis in human polymorphonuclear leukocytes. *Blood.* **91:** 4761–4769.

25. Petyy, H. 2007. Fluorescence microscopy: established and emerging

methods, experimental strategies, and applications in immunology. *Microsc. Res. Tech.* **70:** 687–709.

26. Moss, W., S. Haade, J. M. Lyle, D. A. Agard, and J. W. Sedat. 2005. A novel 3D wavelet-based filter for visualizing features in noisy biological data. *J. Microsc.* **219:** 43–49.

27. Lockwich, T., B. B. Singh, X. Liu, and I. S. Ambudkar. 2001. Stabilization of cortical actin induces internalization of TRP3-associated caveolar Ca^{2+} signaling complex and loss of Ca^{2+} influx without disruption of TRP3-IP3R association. *J. Biol. Chem.* **27:** 27–31.

28. Lockwich, T., X. Liu, B. Singh, J. Jadlowiec, S. Weiland, and I. Ambudkar. 2000. Assembly of Trp1 in a signaling complex associated with caveolin-scaffolding lipid raft domains. *J. Biol. Sci.* **275:** 11934–11942.

29. Brazer, S., B. B. Singh, X. Liu, W. Swaim, and I. S. Ambudkar. 2003. Caveolin-1 contributes to assembly of store operated Ca^{2+} influx channels by regulating plasma membrane localization of TRPC1. *J. Biol. Chem.* **278:** 27208–27215.

30. Lockwich, T., X. Liu, B. B. Singh, J. Jadlowiec, S. Wieland, and I. S. Ambudkar. 2000. Assembly of Trp1 in a signaling complex associated with caveolin-scaffolding lipid raft domains. *J. Biol. Chem.* **275:** 11934–11942.

31. Carafoli, E. 2002. Calcium signaling: a tale for all seasons. *Proc. Natl. Acad. Sci. USA.* **99:** 1115–1122.

32. Unser, M., and A. Albroubi. 1996. A review of wavelets in biochemical applications. *Proc. IEEE.* **84:** 626–638.

33. Malik, Z., G. M. Denning, and D. J. Kusner. (2000) Inhibition of Ca^{2+} signaling by *Mycobacterium tuberculosis* is associated with reduced phagosome-lysosome fusion and increased survival within human macrophages. *J. Exp. Med.* **191:** 287–302.

34. Montell, C., L. Birnbaumer, V. Flockerzi, R. J. Bindels, E. A. Bruford, M. J. Caterina, D. E. Clapham, C. Harteneck, S. Heller, D. Julius, et al. 2002. A unified nomenclature for the superfamily of TRP cation channels. *Mol. Cell.* **9:** 229–231.

35. Hinkovska-Galcheva, V., L. Boxer, P. Mansfield, D. Harsh, A. Blackwood, and J. A. Shayman. 1998. The formation of ceramide-1-phosphate during neutrophil phagocytosis and its role in liposome fusion. *J. Biol. Chem.* **273:** 33203–33209.

36. Sawyer, D., J. A. Sullivan, and G. L. Mandell. 1985. Intracellular free calcium localization in neutrophils during phagocytosis. *Science.* **230:** 663–666.

37. Murata, T., J. A. Sullivan, D. W. Sawyer, and G. L. Mandell. 1987. Influence of type and opsonization of ingested particle on intracellular free calcium distribution and superoxide production by human neutrophils. *Infect. Immun.* **55:** 1784–1791.

38. Dewitt, S., W. Tian, and M. B. Hallett. 2006. Localized PtIns (3,4,5)P3 or PtIns (3,4)P2 at the phagocytic cup is required for both phagosome closure and Ca^{2+} signaling in HL60 neutrophils. *J. Cell Sci.* **119:** 443–451.

39. Ambudkar, I., S. C. Brazer, X. Liu, T. Lockwich, and B. Singh. 2004. Plasma membrane localization of TRPC channels: role in caveolar lipid rafts. *Novartis Found. Symp.* **258:** 63–70.

40. Mitsutake, S., and Y. Igarashi. 2005. Calmodulin is involved in the Ca^{2+}-dependent activation of ceramide kinase as a calcium sensor. *J. Biol. Chem.* **280:** 40436–40441.

41. Clapham, D. 2003. TRP channels as cellular sensors. *Nature.* **426:** 517–523.

42. Kiselyov, K., X. Xu, G. Mohayeva, T. Kuo, I. N. Pessah, G. A. Mignery, X. Zhu, L. Birnbaumer, and S. Mauallem. 1998. Functional interaction between InsP3 receptors and store-operated Htrp3 channels. *Nature.* **396:** 478–482.

43. He, L-P., T. Hewavitharana, J. Soboloff, M. A. Spassova, and D. L. Gill. 2005. A functional link between store-operated channels revealed by the 3,5,-bis(trifluoromethyl)pyrazole derivative BTP2. *J. Biol. Chem.* **280:** 10997–11006.

44. Itagaki, K., K. B. Kannan, D. H. Livingston, E. A. Deitch, Z. Fekete, and C. J. Hauser. 2002. Store-operated calcium entry in human neutrophils reflects multiple contributions from independently regulated pathways. *J. Immunol.* **168:** 4063–4069.

45. Hauser, C., Z. Fekete, D. H. Livingston, J. Adams, M. Garced, and E. A. Deitch. 2000. Major trauma enhances store-operated calcium influx in human neutrophils. *J. Trauma.* **48:** 592–597.

46. Mitsutake, S., T-J. Kim, Y. Inagaki, M. Kato, T. Yamashita, and Y. Igarashi. 2004. Ceramide kinase is a mediator of calcium-dependent degranulation in mast cells. *J. Biol. Chem.* **279:** 17570–17577.

47. Liu, B., N. Andrieu-Abadie, T. Levade, P. Zhang, L. Obeid, and Y. Hannun. 1998. Glutathione regulation of neutral sphingomyelinase in tumor necrosis factor-induced cell death. *J. Biol. Chem.* **273:** 11313–11320.

48. Shakor, A., K. Kwiatkowska, and A. Sobota. 2004. Cell surface ceramide generation precedes and controls FcgRIIA clustering and phosphorylation in rafts. *J. Biol. Chem.* **279:** 36778–36787.